AD_____

Award Number: DAMD17-99-1-9001

TITLE: Clinical Evaluation of Digital Mammography

PRINCIPAL INVESTIGATOR: Laurie L. Fajardo, M.D.

CONTRACTING ORGANIZATION: The Johns Hopkins University
School of Medicine
Baltimore, Maryland 21205-2196

REPORT DATE: February 2001

TYPE OF REPORT: Annual

PREPARED FOR: U.S. Army Medical Research and Materiel Command
Fort Detrick, Maryland 21702-5012

# REPORT DOCUMENTATION PAGE

Form Approved
OMB No. 074-0188



| 1. AGENCY USE ONLY (Leave blank) | 2. REPORT DATE | 3. REPORT TYPE AND DATES COVERED |
|---|---|---|
| | February 2001 | Annual (01 Feb 00 - 31 Jan 01) |

**4. TITLE AND SUBTITLE**
Clinical Evaluation of Digital Mammography

**5. FUNDING NUMBERS**
DAMD17-99-1-9001

**6. AUTHOR(S)**
Laurie L. Fajardo, M.D.

**7. PERFORMING ORGANIZATION NAME(S) AND ADDRESS(ES)**
The Johns Hopkins University School of Medicine
Baltimore, Maryland 21205-2196

E-Mail: LFAJARDO@jhmi.org

**8. PERFORMING ORGANIZATION REPORT NUMBER**

**9. SPONSORING / MONITORING AGENCY NAME(S) AND ADDRESS(ES)**
U.S. Army Medical Research and Materiel Command
Fort Detrick, Maryland 21702-5012

**10. SPONSORING / MONITORING AGENCY REPORT NUMBER**

**11. SUPPLEMENTARY NOTES**
Report contains color

**12a. DISTRIBUTION / AVAILABILITY STATEMENT**
Approved for Public Release; Distribution Unlimited

**12b. DISTRIBUTION CODE**

**13. ABSTRACT** *(Maximum 200 Words)*

The investigations being conducted under DAMD award 17-999-1-9001 involve a unique group of expert physicists and clinical researchers who have previously collaborated to establish a research group known as the International Digital Mammography Group. Our study entails two aspects of translational research related to the clinical application of digital mammography: technology optimization (Phase 1) & a clinical evaluation (Phase 2).

The technology/system optimization work is near completion and has focused on optimizing the operational parameters most likely to impact mammographic image quality for radiodense breasts (x-ray tube target material, filter composition, tube voltage, and exposure level/radiation dose). Because the dynamic range of x-ray signals recorded with standard screen-film mammography systems is greatly exceeded by digital systems, one of the most promising contributions of digital mammography is improved imaging of moderate to markedly dense breast tissue.

The second phase of this project is a multi-center clinical evaluation comparing optimized digital mammography to SFM in women with moderate or marked breast density who present for problem-solving mammography. Eligible women consenting to participate will undergo a 4-view screen-film and digital mammogram. The primary outcome of interest—lesion detectability on digital versus screen-film mammograms—will be evaluated based on a receiver operating characteristic curve analysis of 12 readers' assessments of the likely presence of malignant lesions based on mammographic findings. Secondarily, differences in case management between the two imaging modalities will be measured. Since 7/15/2000, 217 eligible patients have been enrolled in this trial (38 Group 1 patients, 107 Group 2 patients and 64 Group 3 patients), representing 20-25% of the total accrual planned for the study. Preliminary data analysis of the mammographic assessment for the probability of malignancy on lesions with complete date thus far are: definitely not malignant =32 , probably not malignant=59 , possibly malignant=36 , probably malignant=47, and definitely malignant=7. Once full patient accrual is achieved, a formal reader study, correlated with pathology outcomes will be completedt.

**14. SUBJECT TERMS**
digital mammography, breast cancer detection

**15. NUMBER OF PAGES**
20

**16. PRICE CODE**

| 17. SECURITY CLASSIFICATION OF REPORT | 18. SECURITY CLASSIFICATION OF THIS PAGE | 19. SECURITY CLASSIFICATION OF ABSTRACT | 20. LIMITATION OF ABSTRACT |
|---|---|---|---|
| Unclassified | Unclassified | Unclassified | Unlimited |

## Table of Contents

# ANNUAL REPORT FOR AWARD NUMBER DAMD17-99-1-9001

## "CLINICAL EVALUATION OF DIGITAL MAMMOGRAPHY"

## INTRODUCTION:

The investigations being conducted under DAMD award 17-999-1-9001 involve a unique group of expert physicists and clinical researchers who have previously collaborated to establish a research group known as the International Digital Mammography Group. Our study entails two aspects of translational research related to the clinical application of digital mammography: technology optimization (Phase 1) and a clinical evaluation (Phase 2).

The technology/system optimization work is near completion and has focused on optimizing the operational parameters most likely to impact mammographic image quality for radiodense breasts (x-ray tube target material, filter composition, tube voltage, and exposure level/radiation dose). Because the dynamic range of x-ray signals recorded with standard screen-film mammography systems is greatly exceeded by digital systems, one of the most promising contributions of digital mammography is improved imaging of moderate to markedly dense breast tissue.

The second phase of this project is a multicenter clinical evaluation comparing optimized digital mammography to SFM in women with moderate or marked breast density who present for problem-solving mammography. Eligible women consenting to participate will undergo a 4-view screen-film and digital mammogram. Total accrual will be 1075 women with moderately or markedly dense breasts and either (1) a palpable breast lesion scheduled for biopsy, (2) a nonpalpable lesion detected on SFM and scheduled for biopsy, or (3) a nonpalpable lesion detected on SFM and scheduled for diagnostic imaging and mammographic follow-up only. The primary outcome of interest—lesion detectability on digital versus screen-film mammograms—will be evaluated based on a receiver operating characteristic curve analysis of 12 readers' assessments of the likely presence of malignant lesions based on mammographic findings. Secondarily, differences in case management between the two imaging modalities will be measured.

It is anticipated that optimized digital mammography will improve radiologists' detection of breast cancer over screen-film mammography results, which will in turn demonstrate benefits to the patient and the health-care system as a result of more accurately prescribed clinical management and follow-up.

## BODY: RESEARCH ACCOMPLISHMENTS: SUMMARIES YEARS 1 & 2

### PHASE I: Technical evaluations/system optimization:

The specific aims for Phase 1 are as follows:

**Task 1:** Optimize technical parameters for operating DM systems with respect to x-ray beam/image acquisition, dose considerations, and image quality as a function of signal-to-noise ratio.

Task 1a) Identify preliminary exposure techniques for early patient accrual.
Task 1b) Refine the exposure techniques to optimize imaging performance.

**Task 2):** To ensure quality control of the digital mammographic units during clinical image acquisition.

Our goal is to ensure uniform and consistent imaging performance from the digital units at the six clinical sites during clinical image acquisition. Where applicable, performance evaluation is based on existing American College of Radiology (ACR) guidelines for conventional mammography. Because of the specialized nature of the digital mammography systems, some of the tests have been modified and new guidelines for performance have been defined.

***Description of the Digital Mammographic Systems***

**Fischer system**

This system consists of a long, narrow detector that moves in an arc behind the breast in synchrony with a fan-shaped beam of x-rays. The detector consists of a cesium iodide (CsI) phosphor material, coupled to multiple CCD arrays through glass fiber optic tapers. The CCDs are operated in time delay integration (TDI) mode. The images from the individual CCD modules are combined or "stitched" together to form the complete two-dimensional digital mammogram. At this time, Fischer systems have been installed at Brooke Army Hospital, Thomas Jefferson University Hospital, the University of North Carolina at Chapel Hill and Sunnybrook Health Science Centre.

**General Electric system**

This system incorporates an area detector that is the full size of the desired image field. The detector consists of a layer of CsI deposited on a photodiode array formed on an amorphous silicon thin film transistor array. The image is initially acquired as integrated charge in each pixel, and then read out and digitized by activating a set of control and data lines that connect to the pixel transistors from the sides of the array. A GE system is operational at the University of Pennsylvania.

**Trex system**

The current detector incorporates an area array formed as a matrix of 12 (3x4) smaller modules. Each module is composed of a fiber optic taper, which has an input face that is approximately square. The fibers conduct the image, formed by a CsI layer that covers all of the modules, to 12 square format CCDs. The digitized subimages from the CCDs are then stitched together. Trex units are installed at Johns Hopkins, Good Samaritan Hospital, and at UCLA. These systems are second generation prototype systems. A report

of the performance characteristics of the first generation system was published [Williams 1996].

Although these systems differ in their technical details, they have many factors in common. Each uses CsI(Tl) as an x-ray converter. For all three systems, the mechanical patient positioning is similar to that of conventional mammography systems. The x-ray generators and tubes are also similar to those of conventional units, however, the available targets and filters differ among the three. The following table summarizes some of the characteristics of the three systems.

| | FISCHER | GE | TREX |
|---|---|---|---|
| Active Area | 18.1 cm x 23.4 cm | 18.0 cm x 23.0 cm | 19.2 cm x 25.6 cm |
| Image Matrix Size | 3348 x 4340 | 1800 x 2304 (100 μm mode)<br>3600 x 4608 (50 μm mode) | 4800 x 6400 |
| Pixel Size | 54 μm | 100 μm or 50 μm (effective) | 40 μm |
| X-ray Targets | Tungsten | Molybdenum, Rhodium | Molybdenum |
| Filters | Mo, Rh, Cd | Mo, Rh, Al | Mo, Rh |

**Task 1a: Beam Optimization**

Criteria for optimization of tube voltage and external filtration in digital mammography (DM) differ from those used in screen-film mammography. This is because the separation of the processes of acquisition and display in the former permits the contrast of individual structures to be adjusted when the image is viewed. It is therefore possible to detect objects with low subject contrast provided that the image signal to noise ratio (SNR) is adequate. Thus, rather than maximization of contrast within the constraint of acceptable film darkening and patient dose, beam optimization in digital mammography requires maximization of the image SNR, constrained by acceptable patient dose.

The goal of this study is to identify, for each of several currently available DM systems, technique factors that result in the highest SNR per unit radiation dose, and to do so for a range of breast thickness and adipose/fibroglandular ratio. Data from three different early commercial DM systems, located at three different university test sites, are presented here. Each of these sites is participating in a coordinated clinical evaluation of the DM systems, and a major purpose of our study is to provide guidelines for technique factors to be used during the clinical evaluation.

To identify optimum technique factors, we have chosen the following figure of merit (FOM),

$$FOM = (SNR)^2/MGD,$$

where MGD is the mean dose to the glandular portion of the breast, and the SNR is as defined in section 2.2 below. This FOM is independent of exposure (in the x-ray

quantum-limited regime of operation), and has been used previously by others in mammographic beam optimization studies (Jennings et al., 1993; Boone et al., 1990).

A set of customized mammographic phantoms was circulated among the group of physicists at the participating clinical sites. The phantom set consists of blocks of three different fibroglandular/fat breast tissue compositions- 30/70,50/50 and 70/30. One block of each type contains test objects including step wedges of two types (microcalcification and mass equivalent compositions), and several other types of targets.

At each site, 9 different phantoms are tested (3 compositions x 3 thicknesses: 3, 5, and 7 cm). For each phantom, a wide range of kVp, along with all applicable target/filter combinations, is tested. The goal is to find the kVp, target and filtration that will provide the highest signal-to-noise (SNR) for a given dose. We are using the quantity $(SNR)^2/MGD$ as a figure of merit (FOM), where MGD is the calculated mean glandular dose. The signal is taken as the difference between average pixel values in regions of interest (ROIs) centered on steps in the step wedges, and of ROIs in the nearby phantom background area. The MGD for each setup is calculated from the measured half-value layer (HVL), entrance exposure, phantom composition and thickness, kVp and target/filter combination, according to the tables given by Sobol and Wu.

**Initial Results: Data from the TREX Digital Mammography System at Johns Hopkins Medical Institution:**

Following are example plots of measured signal, SNR, and the FOM, as a function of kVp, for a 70/30 fibroglandular/fat equivalent phantom composition, using the signal from the microcalcification-equivalent material. These data were obtained from the DM system at Johns Hopkins. The results of these studies will be presented at the 5th International Workshop on Digital Mammography, Toronto, CA, June 11-14, 2000.

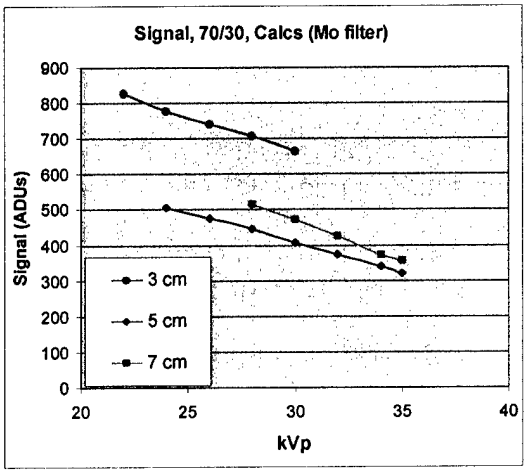


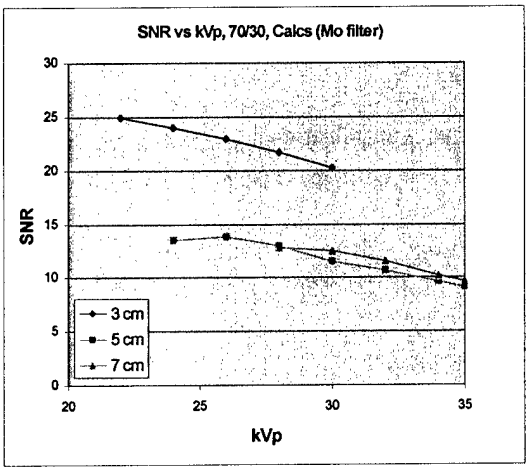

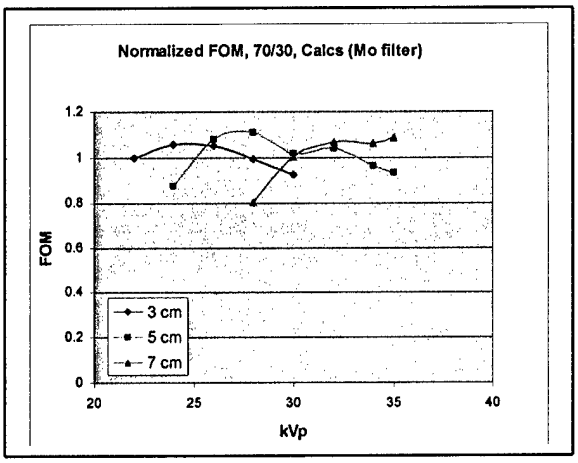


Subsequent Data Acquisition: Three different Digital Mammography (DM) Systems

Three DM units from three different manufacturers were subsequently evaluated and optimized. The units from Fischer, GE, and Trex will hereafter be referred to as Systems 1, 2, and 3, respectively. A common set of phantoms was circulated between the physicists participating in the study. The phantoms were assembled from stacks of blocks of breast equivalent material (CIRS, Inc., Norfolk, VA). Nine different phantoms were assembled and imaged, simulating breasts of three different thicknesses (3 cm, 5 cm, and 7 cm), and three different attenuation equivalent adipose/fibroglandular mass ratios (30/70, 50/50, and 70/30). All blocks of a given phantom had the same adipose /fibroglandular ratio, except for two 5 mm thick blocks, common to all phantoms, that are 100% adipose equivalent. These blocks were placed at the top and bottom of the stack to simulate skin (see figure 1). In each phantom stack assembled, the centrally located block in the stack (the signal block) contained a series of test objects. For the data reported here, the test objects of interest were two stepwedges, one each of calcification equivalent and mass equivalent material. The mass equivalent stepwedge has the same x-ray attenuation as 100% glandular equivalent material, and the microcalcification equivalent step wedge is composed of calcium carbonate. Figure 2 is a schematic of a signal block showing the dimensions of the block and step wedges (other test objects present in the signal block have been omitted for clarity). The thickness of all signal blocks is 2 cm. Images were obtained in manual mode with the phantoms positioned at the chest wall edge of the receptor, centered left to right. Exposure time was selected to give approximately the same average pixel value in the phantom background area for each phantom/technique combination. For each combination two images were obtained with identical exposure times for the purpose of image subtraction, taking care not to move the phantom between the two exposures. At each site, entrance exposures (mR/mAs) and half value layers (HVLs) were measured for each target/filter/kVp combination used.

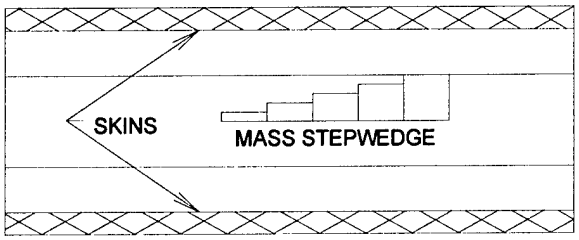


Figure 1: Side view of a 5 cm thick phantom, comprised of one 2 cm thick signal block, two 1 cm thick blank blocks, and two 0.5 cm thick skins.

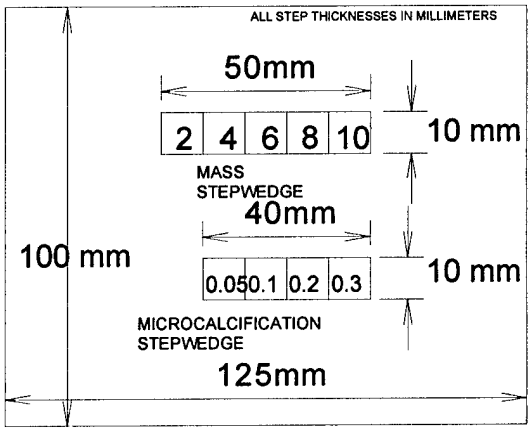


Figure 2: Schematic diagram of a signal block

**Image Analysis:**

Signal was defined as the difference between the average pixel values in a region of interest (ROI) centered on an individual step (but not including the step boundaries), and an equal sized ROI located immediately adjacent to the step, but containing only background. To quantify the image noise, the two images of a given phantom, obtained at a common technique, were subtracted. Image subtraction was performed to

remove fixed pattern noise associated with phantom defects, detector nonuniformity, and the heel effect. Noise in a single image was defined as the rms pixel-to-pixel fluctuations in an ROI of 1109 x 511 pixels in the difference image, divided by the square root of two.

**Calculation of MGD:**

Table I lists each of the target and filter combinations tested in the study. Also given for each target/filter combination are the range of kVps used, and the corresponding HVL

Table I

| Target | Filter | kVp range | HVL range (mm Al) |
|---|---|---|---|
| Molybdenum | Molybdenum | 22-35 | 0.26-0.43 |
| Molybdenum | Rhodium | 24-39 | 0.37-0.51 |
| Rhodium | Rhodium | 25-35 | 0.36-0.52 |
| Tungsten | Aluminum | 29-45 | 0.46-0.77 |
| Tungsten | Rhodium | 32-45 | 0.47-0.58 |

Target/filter combinations, kVp ranges, and HVL ranges of the systems tested. Two of the three mammographic systems used Mo/Mo and Mo/Rh combinations. In those cases, the kVp and HVL ranges given represent the pooled values from both systems.

range. In several cases, the same target/filter combination was available on more than one DM system. Table I lists the combined kVp and HVL ranges from all systems.

The MGD for each phantom was calculated using its known thickness and composition, and the measured HVL and mR/mAs values from each DM system. For Mo/Mo and Mo/Rh spectra, the parameterized dose tables of Sobol and Wu were utilized to obtain the glandular dose per unit exposure (Sobol and Wu, 1997). For the W/Al spectra, normalized (to entrance exposure) MGD values were obtained from the data of Stanton et al. (Stanton et al., 1984). Their data were extrapolated to 3 cm breast thickness, and interpolation between their published HVL curves was used to obtain correction factors for the particular glandular volume fractions (0.22, 0.40, and 0.61, corresponding to glandular mass fractions of 0.30, 0.50, and 0.70, respectively) used in our study. For the W/Rh spectra, the calculations of Boone were utilized, interpolating between his published HVL and adipose/fibroglandular composition values (Boone, 1999). All FOM values were obtained by dividing the square of the SNR by the MGD, expressed in units of $10^{-5}$ Gy (1 mrad).

The measured HVL values for the seven specific target/filter combinations tested at the three sites, as a function of kVp, are shown in Figure 3. Figure 4 shows the corresponding normalized MGD, $D_{gN}$, calculated for each of the seven spectra, plotted versus the measured HVL. Similarly, Figure 5 shows $D_{gN}$ for each target/filter combination tested, plotted versus kVp. The general tradeoff between loss of contrast and reduction in MGD with increasing kVp is illustrated in Figure 6. In this example, the measured contrast of the 0.3 mm thick (thickest) calcification step in shown for the 5 cm thick, 50/50 phantom.

For each of the three DM systems, SNR versus kVp, and the corresponding FOM values vs. kVp have been determined. Figures 7-12 show the results obtained for the 300 micron thick step of the calcification stepwedge in the three 50/50 composition phantoms, for each of the three imaging systems. To illustrate the applicability of these data to objects, the dependence of the FOM on the step thickness for both types of stepwedges is presented in Figures 13 and 14. These data are from images obtained on System 3, using a Mo/Mo target/filter combination to image a 5 cm thick, 50/50 composition phantom. Finally, Figures 15-17 illustrate the effect on the FOM of changing breast composition, holding breast thickness fixed. These data were obtained using System 1, and signals were calculated using the 10 mm thick mass equivalent step.

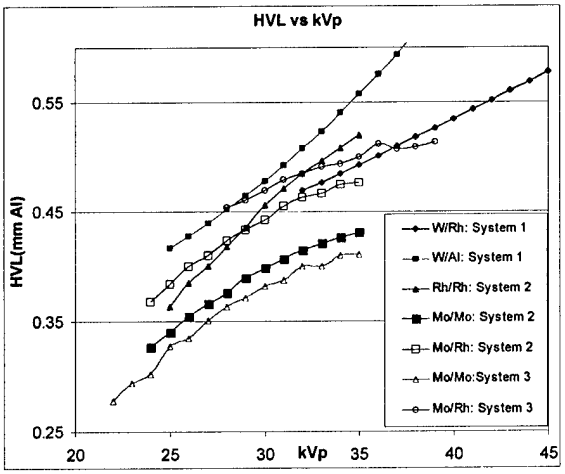


Figure 3: Measured HVLs for the three DM systems, plotted versus kVp.

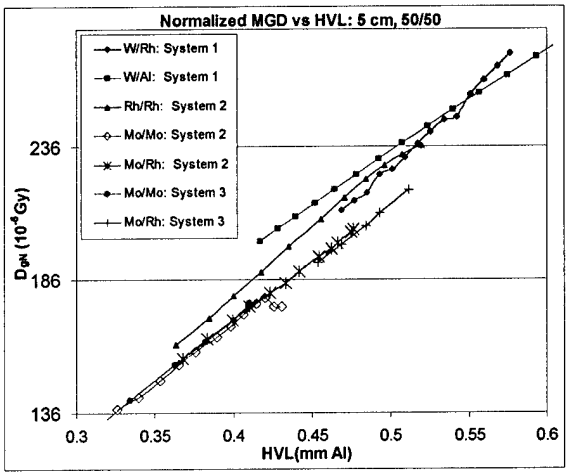


Figure 4: Normalized mean glandular dose versus HVL, for the DM units tested, assuming a 5 cm thick, 50/50phantom.

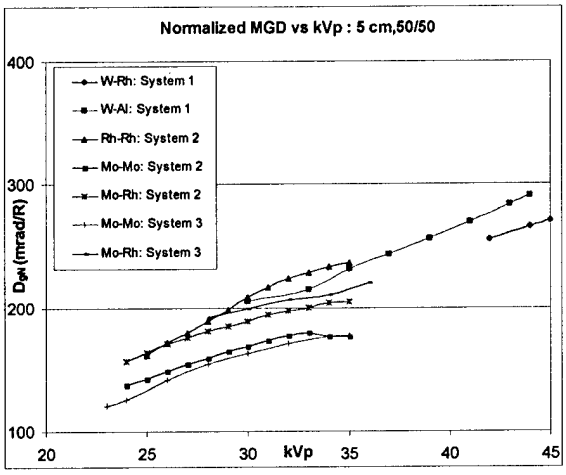


Figure 5: Normalized mean glandular dose vs. kVp for the DM units tested, assuming a 5 cm thick, 50/50 phantom.

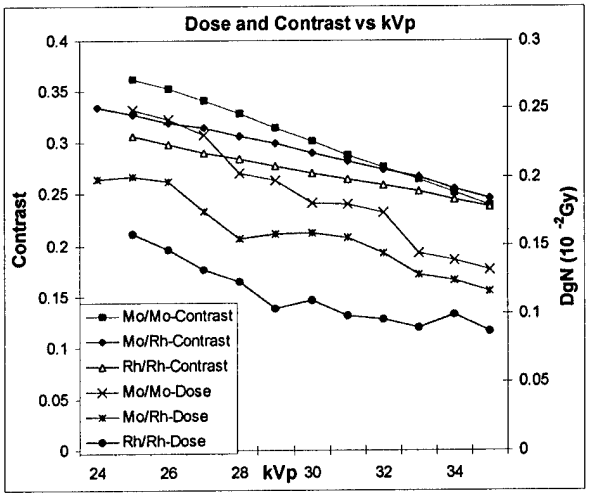


Figure 6: Dose and contrast versus kVp for System 2, using the 0.3 mm calcification step in a 5 cm thick, 50/50 phantom

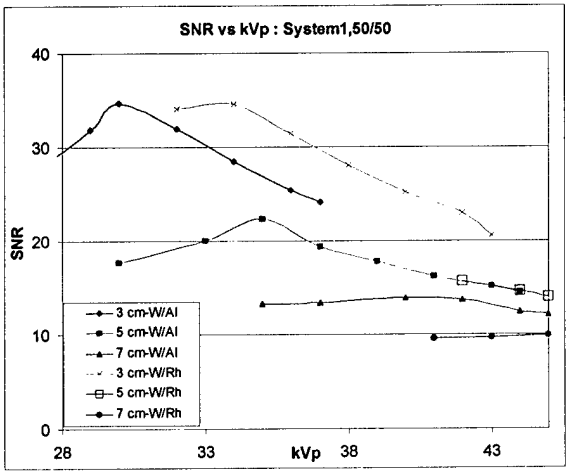


Figure 7: System 1, SNR vs. kVp.

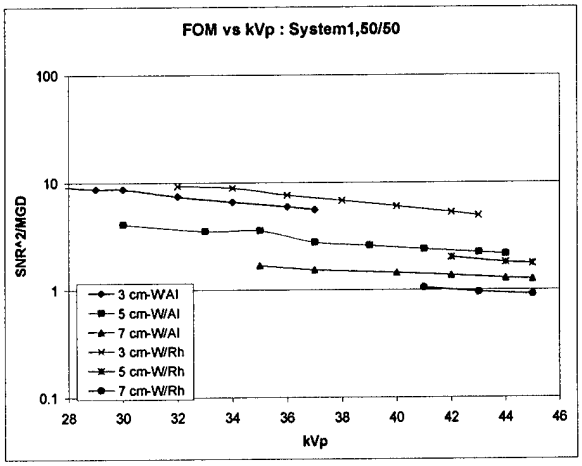


Figure 8: System 1, FOM vs. kVp.

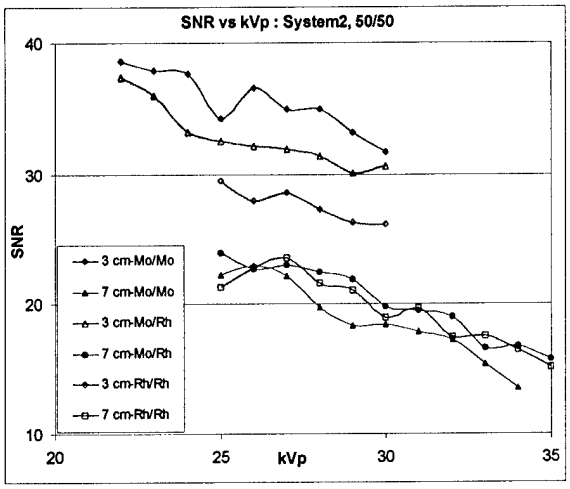


Figure 9: System 2, SNR vs. kVp. 5 cm phantom data have been omitted for clarity, and fall between the 3 cm and 7 cm phantom data shown.

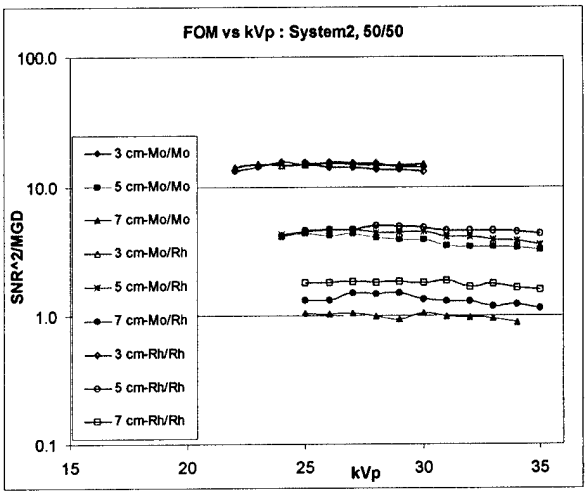


Figure 10: System 2, FOM vs. kVp.

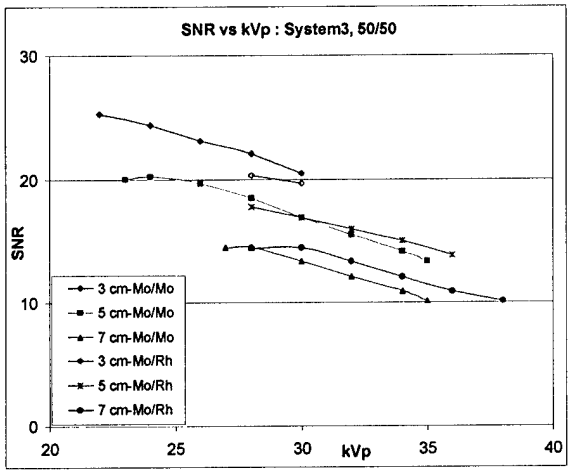


Figure 11: System 3, SNR vs. kVp

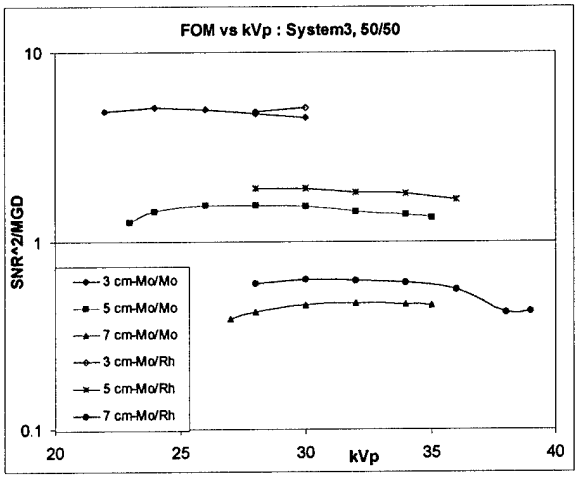


Figure 12: System 3, FOM vs. kVp.

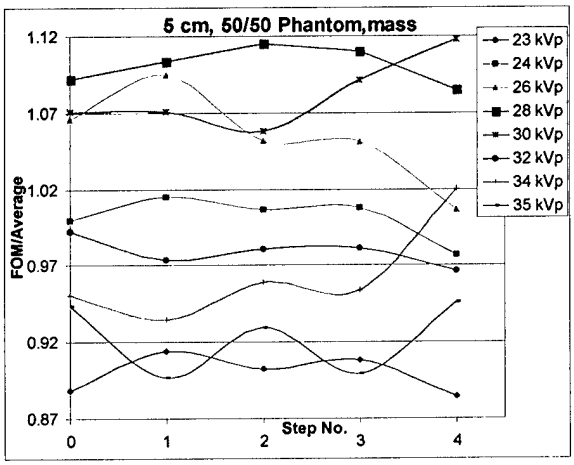


Figure 13: FOM values for the five steps of the mass stepwedge, normalized by the average value for each step. The average FOM values ranged from 0.2 (step 0) to 0.011 (step 4). Data are from System 3, imaging the 5 cm 50/50 phantom.

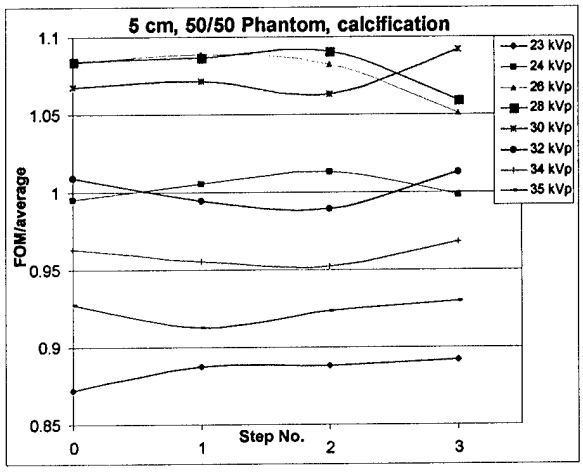


Figure 14: FOM values for the four steps of the calcification stepwedge, normalized by the average value for each step. The average FOM values ranged from 1.4 (step 0) to 0.64 (step 3). Data are from System 3, imaging the 5 cm 50/50 phantom.

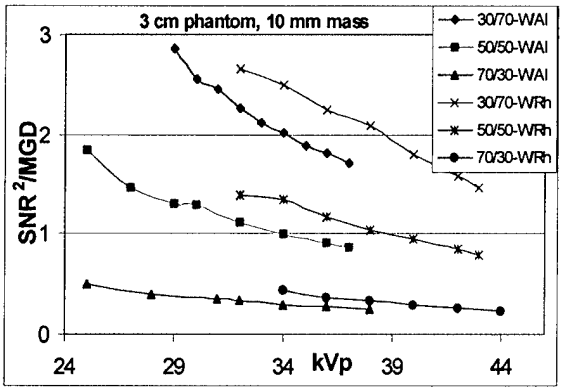


Figure 15: FOM vs kVp for 3 cm thick phantoms of three compositions, imaged on System 1.

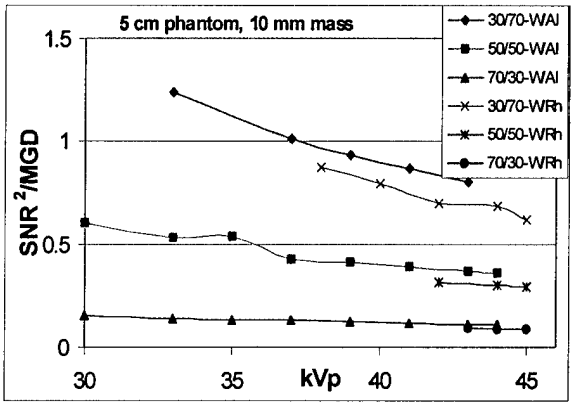


Figure 16: FOM vs kVp for 5 cm thick phantoms of three compositions, imaged on System 1.

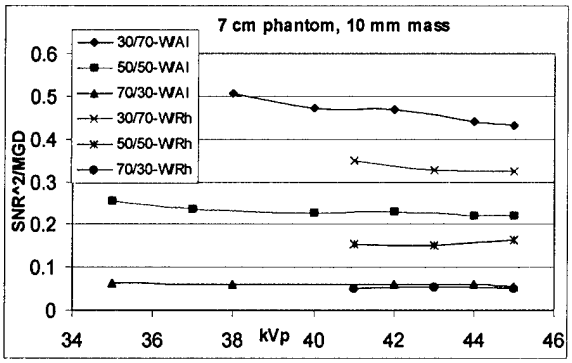


Figure 17: FOM vs kVp for 7 cm thick phantoms of three compositions, imaged on System 1.

**Task 2: Quality Control:**
We have developed and tested several new phantoms and test tools for quality control of DM systems. Description and preliminary results from application of these tools has been presented at the 1998 RSNA [Development of a quality control system for full-field digital mammography, MJ Yaffe, MB Williams, LT Niklason, GE Mawdsley, AD Maidment, Radiology 209(P) (1998) 160]. We have appended the current version of the Quality Control Manual in Appendix B.

**Phase II. Clinical Trial: Summary Years 1 & 2**
During year one of this study, a standardized clinical protocol (Protocol Manual was provided as an appendix with the year 1 annual report) was established and institutional IRB approvals and DAMB Human Investigations approvals for all six clinical sites were obtained. In addition, the case report forms for data collection were pilot tested and electronically programmed into laptop computers that were then distributed to the clinical site (the case report/data collection forms were provided as an appendix with the tear 1 annual report). Training sessions on the laptop computers for the research assistants and site radiologist investigators have been completed. Each clinical site has recruited and performed data entry on five clinical "test" cases. The digital mammography archive at Johns Hopkins Medical Institution has been established and tested. All digital mammograms are now being backed up and archived onto CDs, rather than magneto-optical disks as originally planned.

In addition, we have completed the data analysis on the 200 patients we recruited in our pilot study. The clinical trial opened on July 15, 2000; below, we report the accrual progress for the first 16 months of the trial.

**Table 1: No. Eligible (enrolled and non-enrolled) & Disqualified (non-eligible patients enrolled) in Clinical Trial as of November 15,2001**

| Johns Hopkins | | | University of N. Carolina | | | University of Pennsylvania | | | University of Toronto | | | Good Samaritan | | |
|---|---|---|---|---|---|---|---|---|---|---|---|---|---|---|
| ENR | NON | DIS | ENR | NON | DIS | ENR | NON | DIS | ENR | NON | DIS | ENR | NON | DIS |
| 99 | 125 | 28 | 41 | 163 | 16 | 23 | 12 | 1 | 24 | 30 | 7 | 30 | 40 | 2 |

| Aggregate Totals | |
|---|---|
| Enrolled & Eligible | **217** |
| Non-enrolled | **370** |
| Disqualified | **54** |

ENR = enrolled
NON = non-enrolled & potentially were eligible
DIS = enrolled, but found to be ineligible

**Table 2: No. Eligible Patients Accrued in each Study Group as of 11/15/01**

| Johns Hopkins | | | University of N. Carolina | | | University of Pennsylvania | | | University of Toronto | | | Good Samaritan | | |
|---|---|---|---|---|---|---|---|---|---|---|---|---|---|---|
| Study group | | | Study group | | | Study group | | | Study group | | | Study group | | |
| I | II | III | I | II | III | I | II | III | I | II | III | I | II | III |
| 21 | 44 | 29 | 4 | 15 | 22 | 3 | 14 | 6 | 9 | 15 | 0 | 1 | 19 | 7 |
| Unknown = 5 | | | | | | | | | | | | Unknown = 3 | | |

| **Aggregate Totals** | |
|---|---|
| **Group 1** | **38** |
| **Group 2** | **107** |
| **Group 3** | **64** |
| **Unknown** | **8** |
| **TOTAL** | **217** |

**Table 3: Age & Ethnic Distribution of Eligible Patients Among the 5 Participating Clinical Sites as of 11/15/01****

| | Johns Hopkins | University of N. Carolina | University of Pennsylvania | University of Toronto | Good Samaritan |
|---|---|---|---|---|---|
| **AGE** | | | | | |
| | 49.3 | 55.4 | ** | 55.4 | ** |
| **RACE** | | | | | |
| White | 75 | 2 | ** | 2 | ** |
| Black | 39 | 31 | ** | 16 | ** |
| Other | 4 | 2 | ** | 1 | ** |
| ** data analysis incomplete | | | | | |

**Table 4: Breast Parenchymal Radiodensity of Eligible Patients Among the 5 Participating Clinical Sites as of 11/15/01****

| | Johns Hopkins | University of N. Carolina | University of Pennsylvania | University of Toronto | Good Samaritan |
|---|---|---|---|---|---|
| **Breast Density** | | | | | |
| Heterogeneously Radiodense | 93 | 31 | ** | 16 | ** |
| Extremely Radiodense | 33 | 4 | ** | 4 | ** |
| ** data analysis incomplete | | | | | |

| Table 5: Breast Lesion Type Among Eligible Patients In the 5 Participating Clinical Sites as of 11/15/01** | | | | | |
|---|---|---|---|---|---|
| | Johns Hopkins | University of N. Carolina | University of Pennsylvania | University of Toronto | Good Samaritan |
| **LESION TYPE** | | | | | |
| Mass | 72 | 16 | ** | 11 | ** |
| Asymmetric Density | 23 | 11 | ** | 3 | ** |
| Architectural Distortion | 15 | 1 | ** | 2 | ** |
| Calcifications | 33 | 7 | ** | 8 | ** |
| ** data analysis incomplete | | | | | |

| Table 6: Mammographic Assessment: Breast Lesions Among Eligible Patients in the 5 Participating Clinical Sites as of 11/15/01** | | | | | | |
|---|---|---|---|---|---|---|
| **Mammographic Assessment: Probability of Malignancy** | Johns Hopkins | University of N Carolina | University of Pennsylvania | University of Toronto | Good Samaritan | **Total** |
| Definitely not | 25 | 7 | ** | 0 | ** | 32 |
| Probably not | 37 | 21 | ** | 1 | ** | 59 |
| Possibly malignant | 17 | 6 | ** | 13 | ** | 36 |
| Probably malignant | 41 | 1 | ** | 5 | ** | 47 |
| Definitely malignant | 6 | 0 | ** | 1 | ** | 7 |
| ** data analysis incomplete | | | | | | |

## Key Research Accomplishments:

**PHASE I: Technical evaluations/system optimization:**

- Phase I technical evaluations are completed and optimization work is nearly complete for the three types of digital mammography systems that will be used in the clinical trial.

- A detailed manual has been written that describes the qualitative tests that should be performed by a qualified physicist prior to accepting a particular digital mammography system for clinical use. Such evaluations are critical as this new technology diffuses into routine clinical use. Due to the complexities of digital imagers and their distinct differences from conventional film imagers, it is likely that variability in manufacture and performance will exist. Radiologists and physicists must be aware of these issues and understand how their particular system performs relative to the benchmarks our research group is establishing. We plan to publish a complete guideline on acceptance testing after an

additional year of monitoring performance and quality assurance measurements on all systems utilized in our study.

- The manual devised for this research study also details quality control procedures for digital mammography. This is an obvious and important parameter to control in our study. Additionally, it is likely that digital mammography will be regulated nationally, similar to current regulatory programs for conventional mammography. Thus, our research group will be in a unique position to spearhead these efforts.

**PHASE II: Clinical Trial:**

- At the time of this report, the clinical trial has been open to accrual of patients for 16 months. The expected accrual at this time should be 50% of the total accrual, but only one site, Johns Hopkins has met their accrual expectations. Reasons for accrual delays over the last year have included:
    - One clinical site (UCLA) was unable to participate in the trial as originally planned.
    - Organizational issues among individual clinical sites. Site principal investigators have overestimated their abilities to meet the accrual objectives that were outlined in their individual subcontracts. Issues of a lack of previous experience in a trial of this depth may also be factors.
    - Some clinical sites have experienced poor reliability of performance of their digital mammography systems and have experienced "down time" for repairs, as reflected by the numbers of patients that were potentially eligible, but not enrolled into this study.
    - One site has had personnel difficulties and had no research assistant for a period of time.
    - The Johns Hopkins IRB underwent federal investigation that resulted in the closure of this trial at that site for 4 months.
- Thus, the current accrual reflects only 25% of the total patients originally planned. To meet the objectives of the clinical trial, the following actions will be/have been taken:
    - Dr. Fajardo, the overall principal investigator has discussed accrual strategies with clinical site investigators and research assistants to improve future performance.
    - Dr. Fajardo is contemplating the addition of other clinical sites to meet accrual objectives in a timely manner. This will be undertaken *only* after appropriate discussions with USAMRMC personnel.
    - Dr. Fajardo **will** submit a request to USAMRMC for a 1-year no-cost extension of this project.

## REPORTABLE OUTCOMES:

**Abstracts & Presentations:**

- The 1999 Radiological Society of North America, Chicago, IL, November 27- December 3, 1999.
- "Development of a quality control system for full-field digital mammography". MJ Yaffe, MB Williams, LT Niklason, GE Mawdsley, AD Maidment, Radiology 209(P) (1999) 160.

- The 5th International Workshop on Digital Mammography, Toronto, CA, June 11-14, 2000: "Beam Optimization for Digital Mammography". MB Williams, M More, V Venkatakrishnan, L Niklason, MJ Yaffe, G Mawdsley, A Bloomquist, A Maidment, D Chakraborty, C Kimme-Smith, LL Fajardo.
- "Accuracy of digital mammography vs. screen-film mammography in a diagnostic mammography population". The International Digital Mammography Group

**Manuscripts in Preparation:**
Two manuscripts, authored by the International Digital Mammography Group and reporting data from the pilot study that preceded this Clinical Translational Research Trial have been published:

1. Pisano ED, Cole EB, Hemminger BM, Yaffe MJ, Johnston RE, et al. Image processing algorithms for digital mammography: A pictoral essay. RadioGraphics 2000;20:1479-1491.
2. Pisano ED, Cole EB, Major S, Zong S, Hemminger BM, et al. Radiologists' preferences for digital mammography display: The international digital mammography development group. Radiology 2000;216(3):820-830.

**Informatics - Databases:**
All digital mammography studies performed in this trial and biopsy results will be backed-up in an archive at Johns Hopkins University. This repository of digital mammograms, the majority of which will be from women who also have pathology information, will provide a rich data set for future studies (e.g., the application of computer assisted diagnosis programs to digital mammograms, etc.).

## CONCLUSIONS:

### PHASE I: Technical evaluations/system optimization:

The analysis of SNR and FOM as a function of kVp, shown in Figures 7-12, indicates that although the image SNR tends to decrease monotonically for all systems with increasing kVp, the accompanying MGD reduction results in fairly flat FOM curves. Note, however, in the case of System 1, the SNR falls at low kVp. This is primarily due to tube loading, since it was not possible to obtain the same exit exposure at all kVps (that is, the tube output was insufficient to compensate for the lower transmission through the phantoms). Thus the falling SNR (and the falling MGD) with decreasing kVp are really consequences of falling exposure.

For a given phantom/technique combination, the SNR, and thus the *magnitude* of the FOM, increases with increasing step thickness for both types of stepwedge. However, the *shape* of the FOM vs. kVp curves for a given target/filter/phantom combination are essentially independent of step thickness, and are similar for mass and calcification equivalent signals. This is illustrated by the example shown in figures 13 and 14. This implies that the result of the optimization is not sensitively dependent on signal amplitude.

Figures 15-17 illustrate that, at least in the case of System 1, there is a clear advantage to using rhodium filtration for thin breasts, but that for breasts 5 cm or thicker, aluminum filtration

becomes increasingly advantageous. Similar statements can be made for the molybdenum target systems tested, where molybdenum filtration was superior for 3 cm phantoms of all compositions, but rhodium filtration produced better results for 5 and 7 cm thick phantoms of all compositions. These data suggest that the choice of external filtration is potentially more significant in determination of the overall FOM of a DM system than is choice of tube voltage.

Fahrig and Yaffe developed a model for optimizing spectral shape in digital mammography, and used it to calculate kVp values producing maximum SNR at a fixed dose for W and Mo spectra (Fahrig and Yaffe, 1994). They found that, for a fixed MGD of 0.6 mGy (60 mrads), the peak SNR occurred in the 24-31 kVp range (W spectrum) and 25-29 kVp range (Mo spectrum) for 4 – 8 cm breast thickness, and 50/50 breast composition. Their results were the same, whether the lesion type modeled was infiltrating ductal carcinoma or microcalcification.

Jennings et al. used a computational approach to identify maximum FOM values (FOM = $SNR^2/MGD$) for a variety of target/filter combinations, and breast thicknesses. They found that for a Mo/Mo beam used to image 3-6 cm, 50/50 breasts, the FOM peaks at 27-28 kVp, and changes slowly with changing kVp near the peak values. Very similar FOM vs. kVp curves were obtained for Mo/Mo, Mo/Rh, and W/Al spectra, applied to 6 cm thick, 50/50 composition breasts. The general trends in our data appear to be consistent with those of these previous studies.

Using the data from these measurements, the expert physicists collaborating in this study have designed operating parameters and quality control guidelines that maintain and control peak performance for each of the 3 different types of digital mammography systems that will be used in our clinical evaluation. Our Phase 1 results demonstrate that successful system optimization and quality control of digital mammography systems can be efficiently achieved in a manner similar to conventional screen-film mammography.

**PHASE II: Clinical Trial:**
Laptop computers, programmed with the data collection forms (submitted with prior annual report), have been provided to each of the five clinical sites. Several training session, conducted by telephone conference calls, have been conducted to train the research assistants at each site. Each site has successfully "enrolled" 5 test cases and the clinical trial opened on July 15, 2000.

Since 7/15/2000, 217 eligible patients have been enrolled in this trial (38 Group 1 patients, 107 Group 2 patients and 64 Group 3 patients), representing 20-25% of the total accrual planned for the study. With a one-year no-cost extension of this trial, complete accrual should be achieved.

## REFERENCES:

Boone, J. (1999). Glandular breast dose for monoenergetic and high-energy x-ray beams: Monte Carlo assessment. Radiology 213, 23-37.

Boone, J., Shaber, G., and Tecotzky, M. (1990). Dual energy mammography: A detector analysis. Med.Phys. 17, 665-675.

Fahrig, R. and Yaffe, M. (1994). Optimization of spectral shape in digital mammography: Dependence on anode material, breast thickness, and lesion type. Med.Phys. 21, 1473-1481.

Jennings, R.L., Quinn, P.W., Gagne, R.M., and Fewell, T.R. (1993). Evaluation of x-ray sources for mammography. Proc SPIE 1896, 259-268.

Sobol, WT and Wu, X. Parameterization of mammography normalized average glandular dose tables. Medical Physics 24(4), 547-555. 1997.

Stanton, L., Villafana, T., Day, J., and Lightfoot, D. (1984). Dosage evaluation in mammography. Radiology 150, 577-584.